2015

Analysis and simulation of keyhole formation in micro laser welding

Harish Vadde

ABSTRACT

ANALYSIS AND SIMULATION OF KEYHOLE FORMATION IN MICRO LASER WELDING

Harish Vadde, M.S.
Department of Mechanical Engineering
Northern Illinois University, 2015
Dr. Meung Kim

The purpose of this study is to simulate a finite element model of keyhole formation in micro laser welding and to find out the effects of several parameters including laser beam intensity on the final shape of keyhole formed after welding characterized by width, height of cut and HAZ. A 3D steady state and transient thermo-fluid models of micro laser welding are developed separately in finite element analysis software Ansys and formation of keyhole is monitored continuously. The model is developed considering two phases, liquid metal and solid metal. Boundary conditions are taken in general include convection and heat flux of laser beam. The work material considered is ANSI 304 stainless steel. Finally the simulated results are compared with the experimental values and the results are validated.

NORTHERN ILLINOIS UNIVERSITY
DEKALB, ILLINOIS

AUGUST 2015

ANALYSIS AND SIMULATION OF KEYHOLE FORMATION IN MICRO LASER WELDING

BY

HARISH VADDE

A THESIS SUBMITTED TO THE GRADUATE SCHOOL IN PARTIAL FULFILLMENT OF THE REQUIREMENTS

FOR THE DEGREE

MASTER OF SCIENCE

DEPARTMENT OF MECHANICAL ENGINEERING

Thesis Director:
Dr. Meung Jung Kim

ACKNOWLEDGEMENTS

I would like to express my sincere gratitude to my thesis director Dr. Meung Kim for his continuous support and guidance in this thesis work as well as throughout my graduate study.

I would like to thank Dr. Jenn Terng Gau and Dr. Pradip Majumdar for serving as members of my thesis committee.

I would like to thank my parents and my brother Naresh Vadde for their unconditional love, continuous support, enduring patience and encouragement throughout my journey. Finally, I would like to thank my friends especially Sai Krishna Bobba and everyone who has directly or indirectly helped me for their cooperation in completing the thesis.

DEDICATIONS

To my Family members, Friends with love and gratitude.

TABLE OF CONTENTS

Page

Chapter Page

LIST OF TABLES

Table Page

LIST OF FIGURES

Figure Page

Figure Page

CHAPTER 1

INTRODUCTION

1.1 Laser welding

Welding is a process (or) a technique used to join similar (or) dissimilar metals (or) thermoplastics together by causing fusion. There are different types of welding methods based on the energy sources used. Some of the energy sources used are flame, laser, electric arc, friction, electron beam and ultrasound [1].

Laser beam welding is used to join multiple metal pieces using a laser beam. Laser welding is widely used because of its distinct characteristics like concentrated heat source, small Heat Effected Zone(HAZ), high weld quality, high welding rates, allowing for narrow and deep welds. As a result this process is frequently used in high volume applications like in the ship building, electronic and automotive industry [2].

1.2 Conduction and keyhole type welding

Based on the laser beam power density (beam intensity) used for welding, laser welding is divided into two types they are “conduction mode” and “keyhole mode”. Power Intensity is defined as the ratio of laser beam power to focused area of the laser spot [3].

In conduction mode welding [3], the beam power density is only enough to melt the metal but not to evaporate. So weld infiltration is accomplished just by conduction of heat

down into metal from the surface. In conduction welding the incident beam absorption coefficient is very less compared to the keyhole mode because of the single reflection of incident laser beam on the surface. The figure 1 will clearly explains you the conduction mode welding. In conduction welding the weld bead width to depth ratio is high.

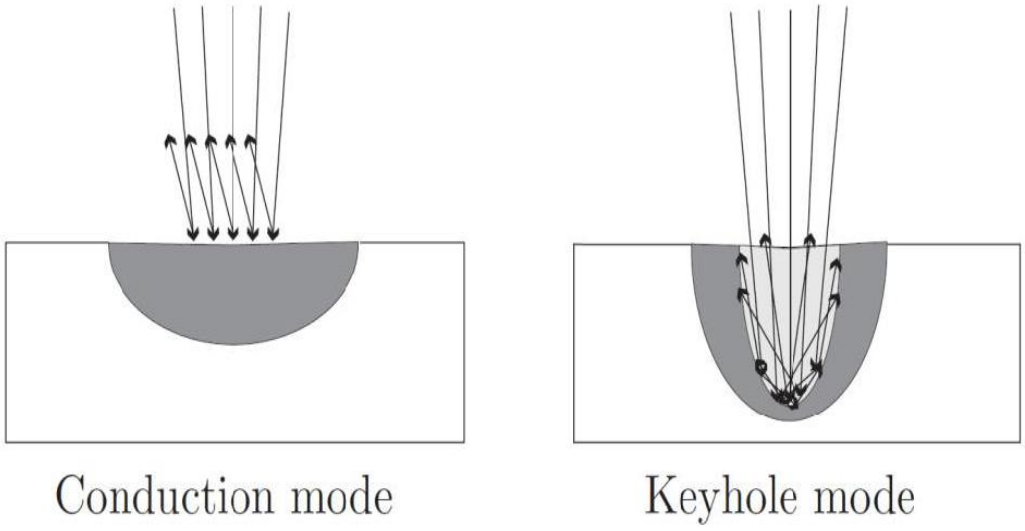

Figure 1: conduction and keyhole mode welding [2].

In Keyhole mode welding the weld penetration is achieved in a different manner. Usually the higher power density laser welding leads to keyhole mode welding [3]. In this welding the metal is heated beyond the melting temperature and converted into vapor. Due to the sudden vaporization, the metal produces pressurized gases which tend to penetrate the molten metal. It helps the laser beam to pass deeper into the metal, making a narrow (or) thin hole known as key hole. From the works of Xie [4] it is proven that due to the effect of multiple reflections of the incident laser beam inside keyhole, the absorption power of incident laser beam energy is increased by more than 90% compared to conduction type welding. Figure 2 clearly explains the

theory of multiple reflections inside the keyhole. The weld bead width to depth ratio in keyhole welding is very less forming a narrow weld.

The below figure 2 shows the development of keyhole experimentally at different times. Development of keyhole or penetration of keyhole depends on the power density and time. With increase in time the keyhole develops deeper.

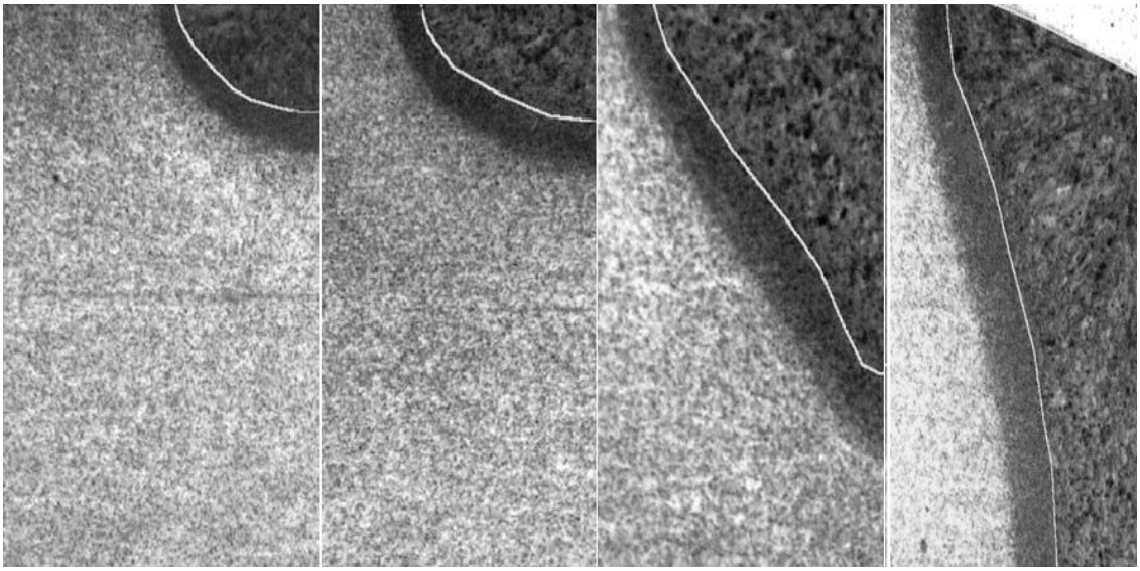

Figure 2: Development of keyhole at different time periods [4].

1.3 Literature review

Maiti [4] designed a 2D transient axisymmetric mathematical Finite Element Model (FEM) considering only solid phase of the material and conduction mode heat transfer, then he showed the development of keyhole formation in laser spot welding considering time dependent material properties and proposed that transition from conduction to keyhole modes is a function

of laser power and time. Then He validated the simulated results by comparing them with experimental values.

Siva Shanmugam [6] and two others developed a 3D Gaussian moving type heat source FEM using SYSWELD software considering only conduction mode of welding and he studied the effect of given input parameters such as beam power, spot diameter, on bead profile and temperature distribution on AISI304 material. He considered that 69.3% of incident beam power is absorbed by the work piece throughout the experiment.

Xie [4] performed many experiments and proposed that work piece surface oxidation increases the absorption power of incident laser beam energy by the work piece greatly and has very small effect on the mechanical properties of welded material after. He also proposed that because of the effect of multiple reflections of the laser beam inside keyhole increases the absorption power of laser beam energy by more than 90% in keyhole mode welding. This effect cannot be seen in only conduction mode welding.

Katiar [7] worked on the joining of dissimilar metals (copper and SS) using Nd: YAG laser welding. He designed a 2D moving Gaussian heat source in FEM software ANSYS and proposed that temperature distribution of work piece mainly depends on thermal properties like conductivity, specific heat and density of the work piece. He also concluded that thermal stresses decreases from the welding zone to fixed side.

Stritt [8] tried to distinguish the two regimes of heat conduction type welding and deep penetration type welding using practical experiments. He found that lower laser power density

levels leads to heat conduction welding whereas the higher levels results in deep penetration welding.

Cho [9] studied the effects of variation of the power intensity of the laser on the diameter and the depth of cut by developing a 3D steady state FEM using ANSYS. He developed simulated model assuming that material has constant thermal properties and incident laser beam intensity is high enough to cause direct evaporation from solid to vapor.

Aditya [10] tried to find out the optimal welding parameters experimentally for AISI304 material using Nd: YAG laser machine and validated the results by developing a conduction mode 3D FEM of laser welding using COMSOL and ANSYS software. He used the temperature independent material properties for developing the model.

1.4 Motivation for thesis

There is a huge increase in usage of laser welding and laser cutting in every field because of its advantages like concentrated heat source, deep welds, high welding rates and good surface finish. By knowing the potential of laser welding a lot of research work is taking place in this field.

If we can predict the weld structure and weld properties before the actual weld by using simulation, we will be able to adjust the welding parameters in order to achieve the desired combination of microstructure and mechanical properties.

Laser welding is complex process involving fluid flows, heat transfer and thermodynamic cycles in very small area in very short time period, so it’s very hard to study experimentally. A FEM model could solve all these limitations. But for now there is no perfect 3D Finite element

model considering all the physics and thermos dynamical cycles. All these things made me to work on this topic.

1.5 Objective of research

The main objective of this research is to

1. Develop a steady state and transient iterative type FE Model of micro laser welding considering two phases of the welded region i.e. solid and liquid phase of metal.
2. Show the development of keyhole.
3. Find out the effects of parameters including laser beam intensity on the final shape of keyhole formed after welding characterized by width, height of cut and HAZ.
4. Validate the simulated results with experimental result and show that simplified assumption of liquid + solid phase gives better simulated results than the only solid phase assumption.

Flow chart of objective:

The objectives are explained in a step-by-step process as shown in following table.

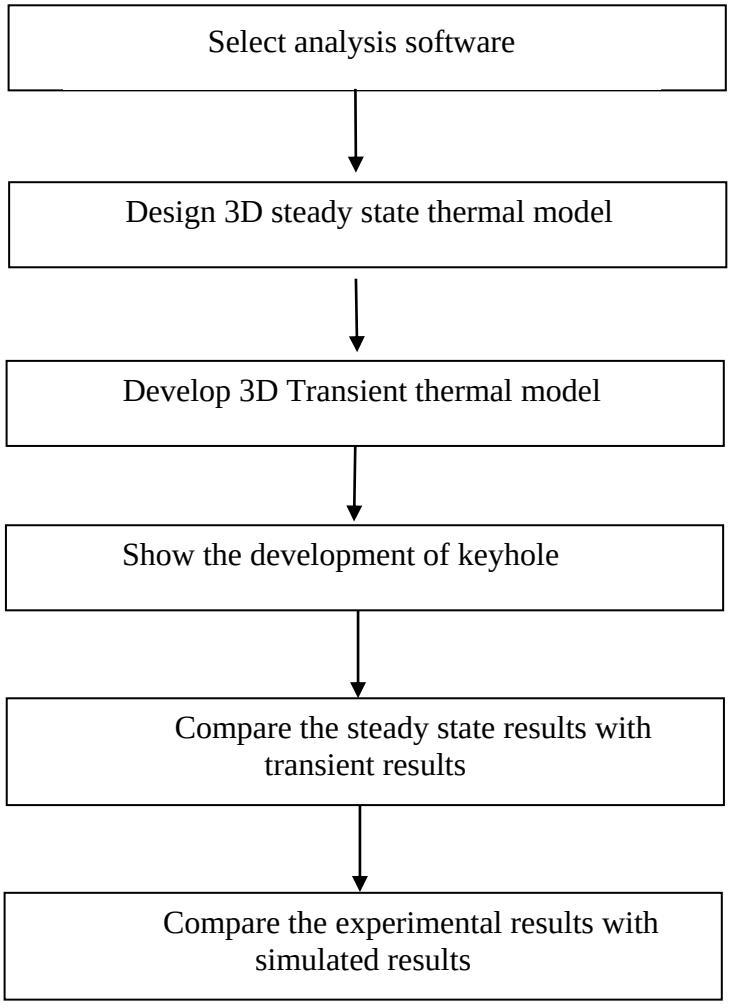

Figure 3: Flow Chart of the objective.

CHAPTER 2

MODELLING OF LASER WELDING

In this chapter, the physical process involved in laser welding and the assumption made while simulating the model are discussed. The boundary conditions, the material properties used and the modelling of heat source used in simulation are also discussed.

2.1 Physical Statement of the model

The physical properties involved in Laser welding are fluidic and thermo dynamical in nature. All this happens in very small area and in short time. When a laser beam strikes the surface of the work piece only some part of the incident beam energy is absorbed by the material and remaining part is reflected. Sometimes the absorbed energy or heat is also lost due to convection and radiation through the material to the surroundings. The amount of incident beam energy absorbed and reflected by the work piece depends on the thermo-physical and optical properties of the material. In this work, Analysis is done on the AISI 304 metal. The schematic representation of the present micro laser welding problem is shown in the figure 4.

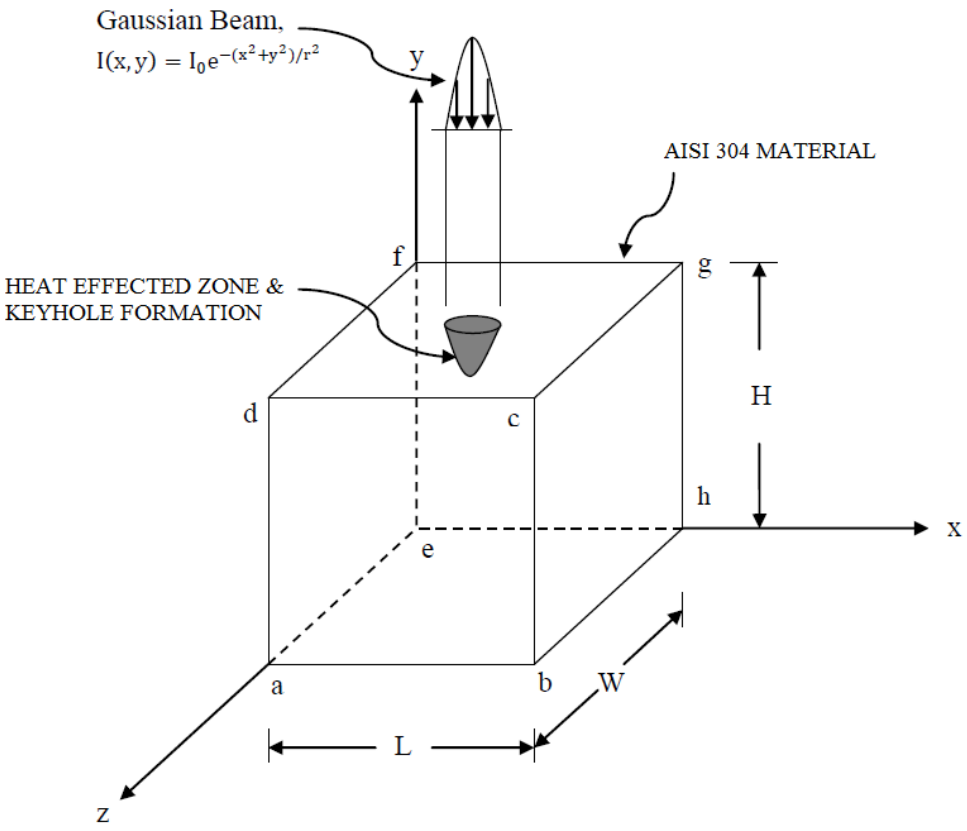

Figure 4: Schematic representation of welding [9].

2.2 Assumptions made in developing the model

The assumptions made while simulating the analysis are as follows:

1) The work piece initial temperature is 22 C, which is the normal room temperature.
2) The heat convection between the weldment and the ambient environments is considered.

3) Only one-half model is simulated due to symmetry to save time.
4) The laser power source is assumed to be a Gaussian beam type.
5) The physical phenomena such as viscous force, buoyancy force and convective melt flow are neglected.
6) Vapor phase during welding is not considered.
7) Material is assumed to be isotropic with temperature dependent thermal properties such as specific heat, thermal conductivity, and density.
8) Melting temperature of the AISI 304 metal is taken as 1400-1450C.[12]
9) The area above the recrystallization temperature i.e. 950 C is taken as Heat affected zone (HAZ).[12]
10) Both the material and incident laser beam are stationary.
11) Simulation is done in iterations.
12) From the second iteration, the part of solid above the melting temperature is made as liquid metal and the simulation is done.
13) Heat absorption coefficient for AISI 304 metal is taken as 31.7% in conduction mode and 54.2% once the liquid metal is formed. These values are taken from works of Xie [4] which will be explained in detailed in the later part of paper.

2.3 Laser Beam heat source modelling

Nonmoving type Gaussian laser beam is chosen as heat source for this simulation. In Gaussian beam heat source, heat flux is distributed radially in all directions. Heat flux is

defined as the rate of heat energy transfer through a unit surface area. Gaussian beam power intensity distribution is given by the following equation [9] [10]:

$I_{(x,y)}$=I_0 ∗e^− ((x^2+y^2)/ r^2)

Where

r = Beam radius

I_0 = Intensity of the laser beam at center

A unit of '*I*' is Watts per meter square.

In Gaussian beam energy distribution, the intensity at center of beam or peak intensity is calculated by following equation:

Intensity at center of beam I_0= P/πr^2

Where

P = power of laser in watts

r = Beam radius

Beam radius (r) for the experiment is taken as 0.0003 M. The Gaussian beam intensity distribution graph is shown in figure 5.

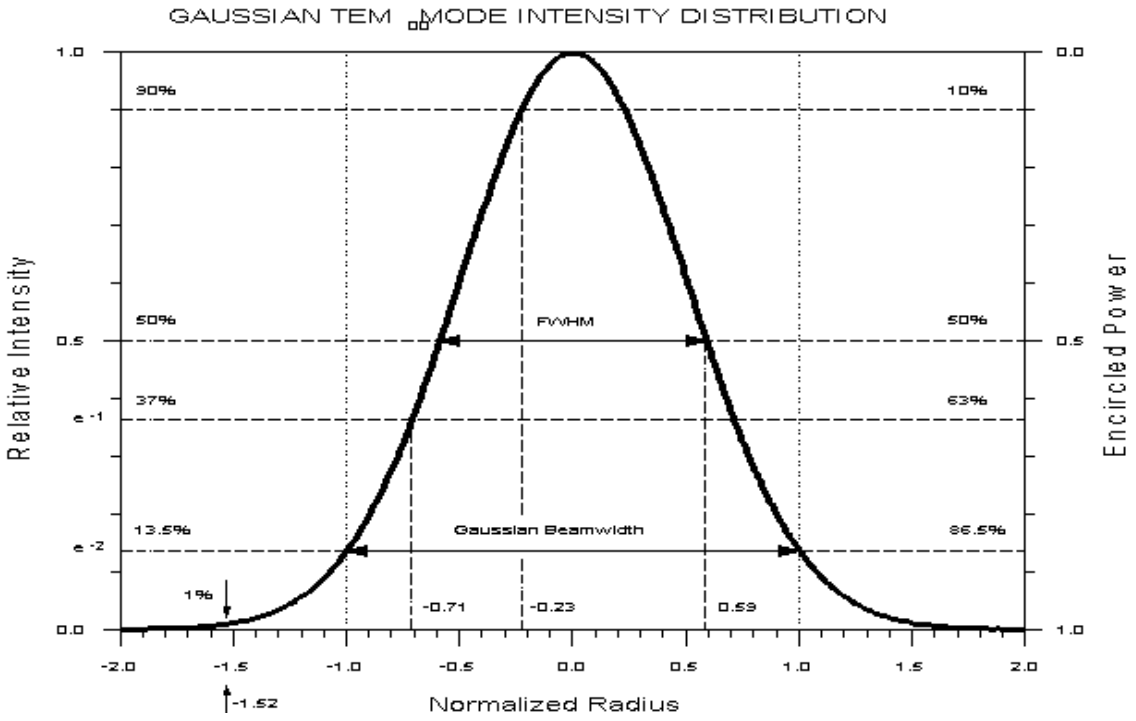

Figure 5: Gaussian beam intensity distribution graph.[12]

2.4 Absorptivity and reflectivity of AISI 304 material

A part of the energy is absorbed by the surface of the work piece when a laser beam falls on it. Some part of it is reflected and remaining part is lost due to convection and radiation to its surroundings. The percentage of energy that is reflected, absorbed and transmitted depends upon the reflectivity (γ), absorptivity (α) and the transitivity (τ) of the material. Relation between is given by following equation [9] [10]:

$$\text{Total beam Intensity } (I_0) = I_\gamma + I_\alpha + I_\tau$$

Where

I_γ = Intensity of beam reflected

I_α = Intensity of beam absorbed

I_τ = Intensity of beam transmitted

The absorptivity power of the material also depends upon the physical state of the work piece material. From the works of Xie [4], it is proven that absorptivity of the material in solid state is less when compared to liquid state of the same material. Multiple reflections of the incident laser beam inside keyhole increase's the absorption of laser energy by more than 90% in keyhole welding. This cannot be observed in conduction mode welding.

Reflectivity coefficient of AISI 304 material for Nd: YAG laser machine with wavelength of 1.06μm at room temperature (solid state) is 69.3% and at Melting temperature (liquid phase) is 55.8% [4]. In this thesis these values are used as the reflectivity coefficient for the simulations. Following table shows you the different reflectivity coefficient values for different materials for different laser welding machines.

Reflectivity of Polished Metals at the Room and Melting Temperatures (%)

	Room Temperature			Melting Temperature (Liquid Phase)		
	CO_2	COIL[a]	Nd:YAG	CO_2	COIL[a]	Nd:YAG
Wavelength (μm)	10.6	1.315	1.06	10.6	1.315	1.06
Aluminum	98.1	94.7	94.1	93.6	81.8	79.8
Copper	98.5	93.6	95.1	94.9	85.5	83.9
Iron	96.9	91.3	90.3	87.0	63.1	58.9
Nickel	95.3	86.6	85.1	89.7	70.8	67.4
Titanium	91.9	76.9	74.3	86.3[b]	61.1[b]	56.7[b]
Carbon Steel	97.3	92.2	91.3	87.9	65.9	61.8
Stainless Steel	90.3	82.4	69.3	86.0[b]	60.3[b]	55.8[b]

Figure 6: Percentage Reflectivity of Materials at the room and melting temperature [4].

2.5 Temperature dependent material properties

The candidature material for this project is AISI 304 stainless steel material. There is no specific reason in choosing this material. Material properties such as thermal and physical properties play a major role in the accuracy of final results in any FEM simulations. Material properties change with the change in temperature. Use of temperature dependent material properties gives exact results. Many researcher use the constant material properties independent of time and temperature. But by knowing the importance of the material properties only temperature dependent material properties are used in this thesis. The temperature dependent material properties of the AISI 304 material are show in the following figure 7.

Temp (K)	Thermal Conductivity, W/m°K	Density , Kg / m³	Specific Heat, J / Kg K	Conv. Coefficient, W/m ²K
200	11	8200	350	8.51
400	15.5	8000	400	25.97
600	19	7800	440	49.9
800	22.5	7600	550	79.3
1000	26	7500	590	113.58
1200	30	7400	610	152.33
1400	34.5	7350	640	192.24
1600	39.5	7300	680	242.07
1800	44	7200	720	292.61
2000	47	7200	760	346.71

Figure 7: Temperature dependent material properties of AISI 304 metal [11].

2.6 Heat Affected Zone (HAZ)

The Heat-Affected Zone is the zone of work piece material, which is not softened (or) melted and has its material properties & microstructure adjusted by welding or heat concentrated cutting operations. The sudden heat from the welding procedure and consequent re-cooling causes this change from the weld interface to the end of the sensitizing temperature in the base metal. The degree of property change depends essentially on the type of material, the filler material used in weld, and the temperature used for welding.

Heat affected zone has lot of importance in the welding process. There is no use if the properties of the material changes completely after the weld. The properties of the material

should remain the same before and after the weld. During weld HAZ should be maintained as small as possible.

In this thesis HAZ is calculated in the simulation based on the recrystallization temperature of the AISI 304 material. The temperature of welded work piece which is above the recrystallization temperature is measured and the obtained area is shown as HAZ. The reference temperature for HAZ is taken as 950 C based on the theories.

1) Based on Fe-Cr phase diagram

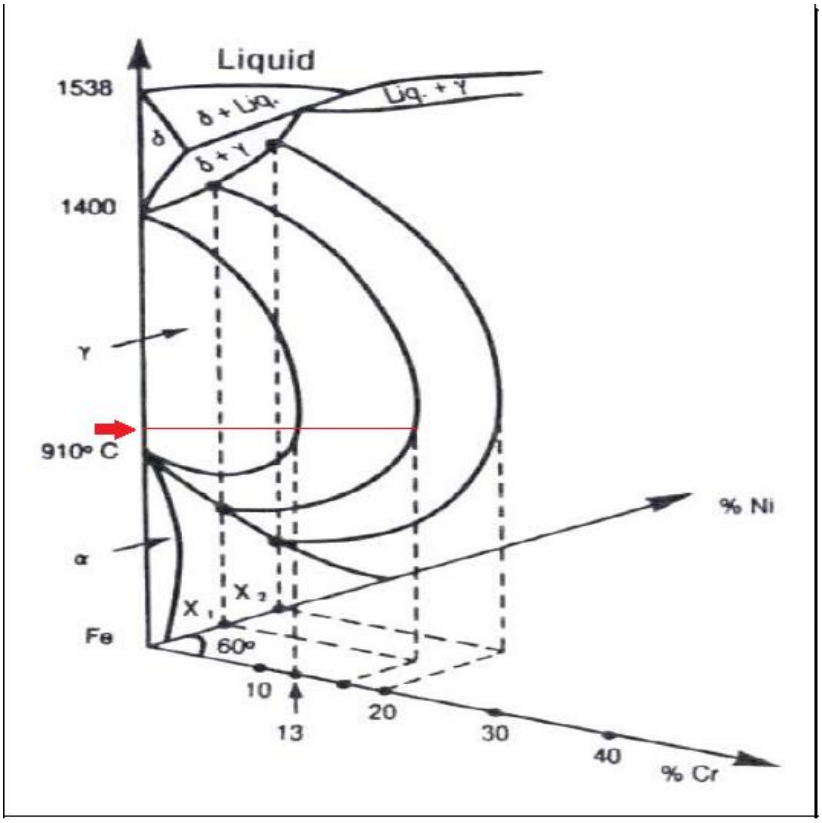

Figure 8: Fe-Ni-Cr 3D Phase diagram [12].

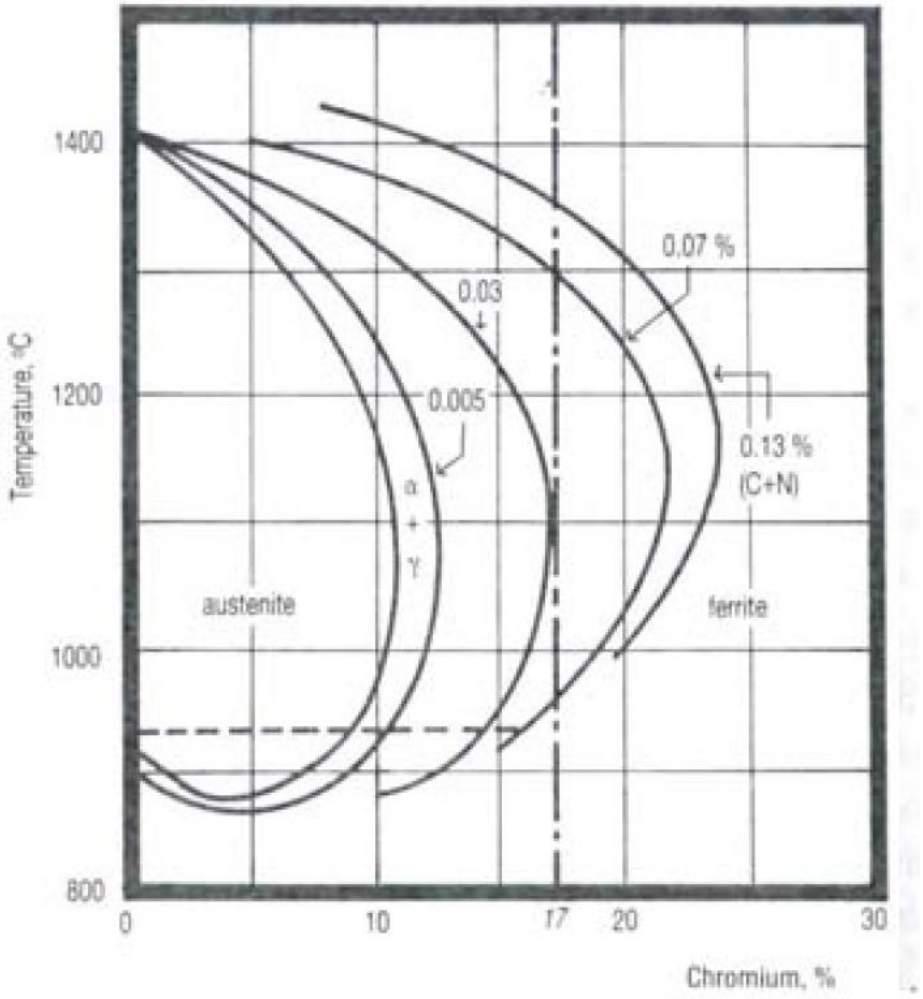

Figure 9: Fe-Cr-C phase diagram [12].

The above figure 8 and 9 shows the AISI 304 metal Fe-Cr phase diagram [12]. For 18% of chromium the phase transition temperature is 950 C. This shows that HAZ temperature range for the AISI 304 material is 950-1450 C. After 1450 C the metal starts melting.

CHAPTER 3

FINITE ELEMENT MODELLING

Finite element modeling is done in Ansys 14.5 software. Ansys workbench and Ansys APDL are combined together to solve the problem.

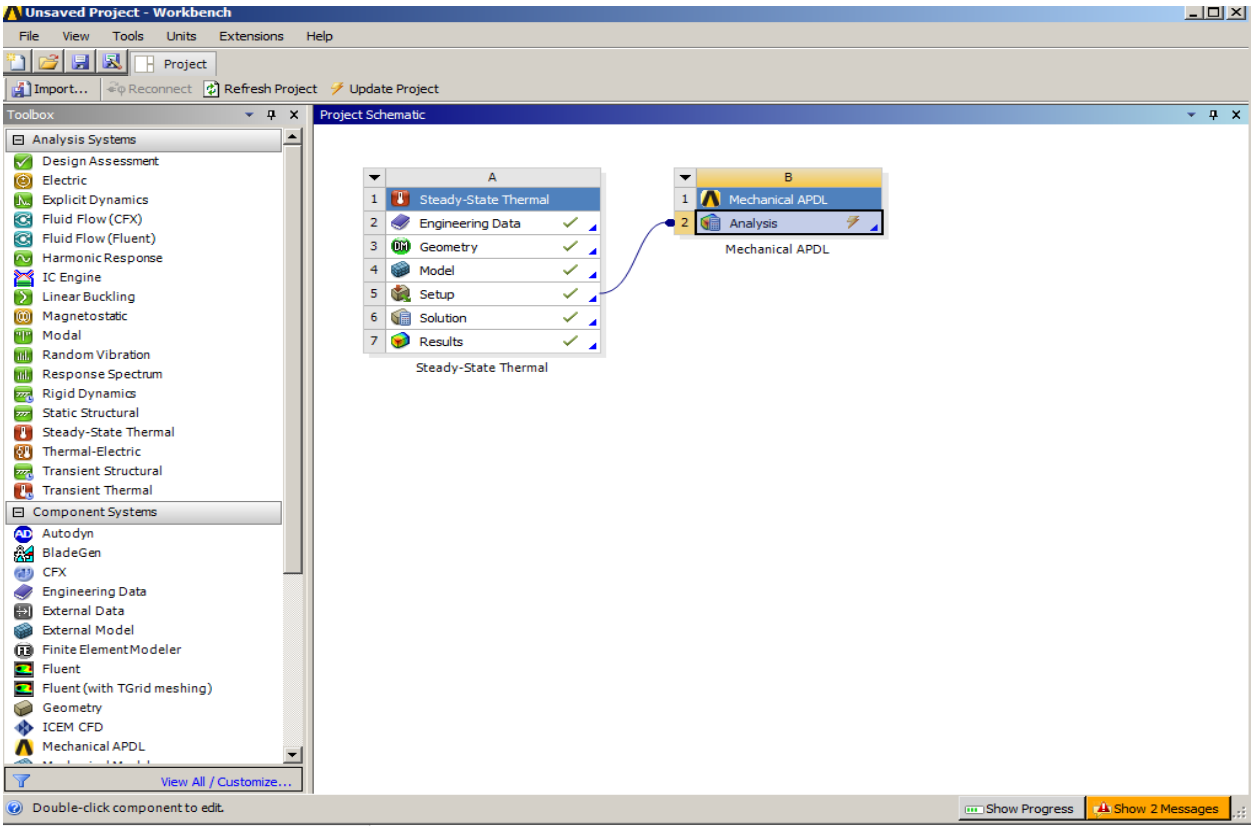

Figure 10: Ansys example window.

3.1 Steady state thermal analysis

A steady state thermal 3D model is developed first and then transient analysis is done. Analysis here is done in iterations till the results converge. In Ansys workbench Steady-State Thermal analysis system is selected. In project schematic window the steady-state thermal table appears. The following inputs are given in the table for solving the problem.

3.1.1 First Iteration

1. Engineering data

Engineering data is the place where material properties are assigned to the work piece in simulation. There are some pre-loaded material libraries in Ansys 14.5 software. If we cannot find the exact material properties in library, we can define the properties manually. Double click the engineering data and the engineering data window appears and then add AISI 304 temperature dependent properties to it. The temperature dependent material properties are shown in 2.5 of chapter 2. For all iterations engineering data remains the same.

2. Geometry

This is the option were the 3D model of work piece is added in Ansys. The work piece for 1^{st} iteration will be a basic rectangular block of dimensions 4×2×0.1 mm. A 3D Rectangular block with those dimensions is designed in the geometry. We can also import .IGES file of the model designed in any other designing software into Ansys workbench. The 3D work piece model is shown below.

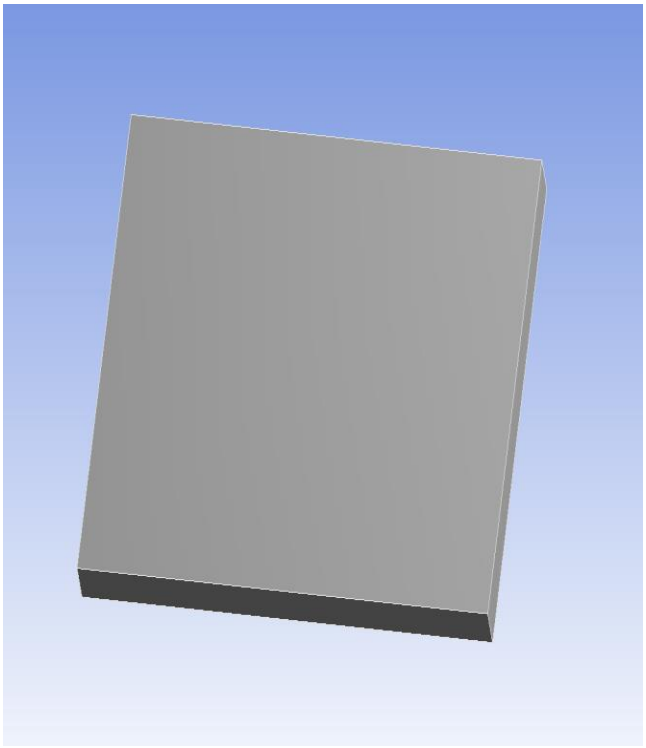

Figure 11: work piece model in Ansys.

3. Boundary conditions

At this step meshing and boundary conditions are given to the model. Give a double click on the setup option. Setup window appears and assign already defined materials to the work piece. Then a very fine meshing is done to the work piece. Accuracy of the result depends on the mesh size. With increase in number of the elements, the accuracy of result increases.

Initially work piece is at room temperature, so the initial temperature of work piece is given as 22 C.

Convection is given to all 6 faces of the work piece because; the work piece loses some energy to surroundings due to convection and radiation. The 6 faces of the work piece are selected and convective heat transfer coefficient of 80 W/m^2 is given as shown in figure 12.

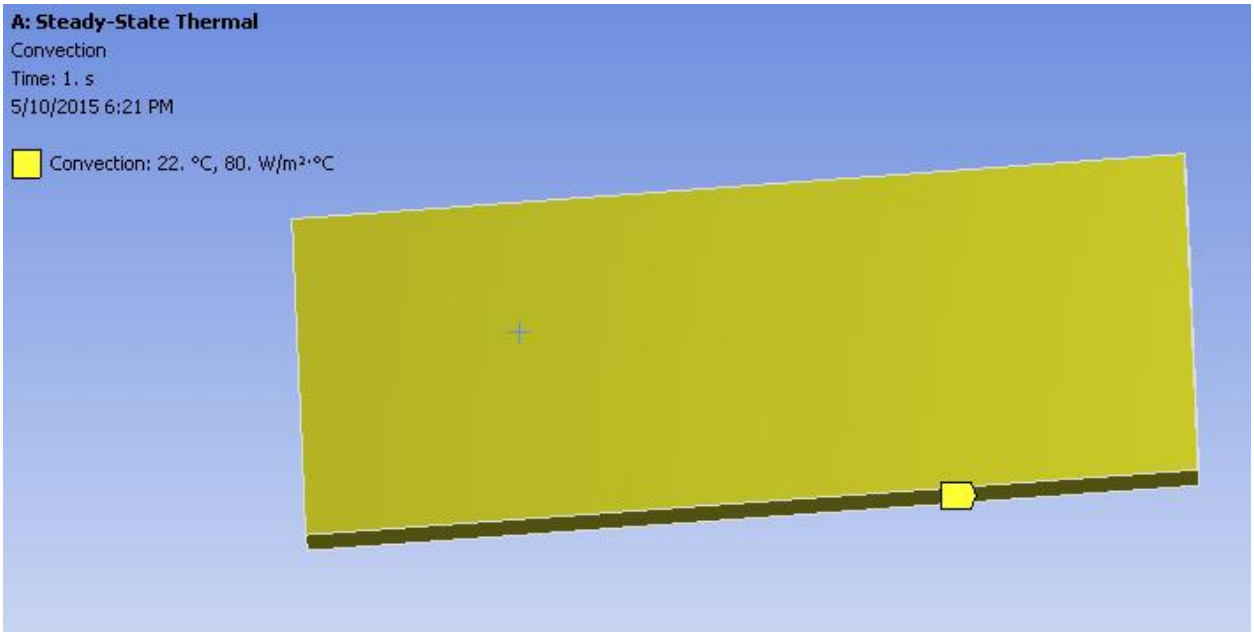

Figure 12: convection boundary condition.

4. Heat flux

The Gaussian heat flux function is defined first and then it is applied on the center of the top face of the work piece. The amount of power absorbed or absorptivity coefficient of work piece is taken as 31.7%, because the work piece is in solid phase. Then the simulation is performed and temperature distribution of the work piece due to heat flux is captured.

Area above the melting temperature i.e. 1450 C is taken as welded region and the parameters like weld width, depth of weld, heat affected zone are measured.

The below figure 13, 14 show the temperature distribution of work piece for the 120W laser power is applied.

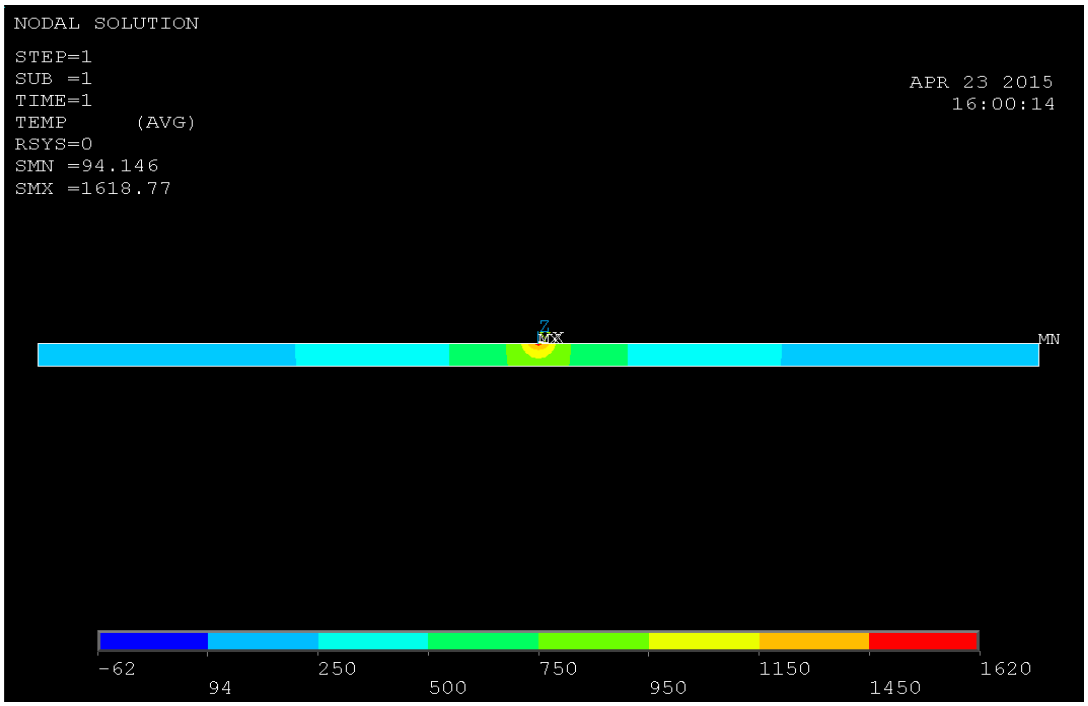

Figure 13: Steady state 1st iteration temperature distribution on work piece for 120W laser power.

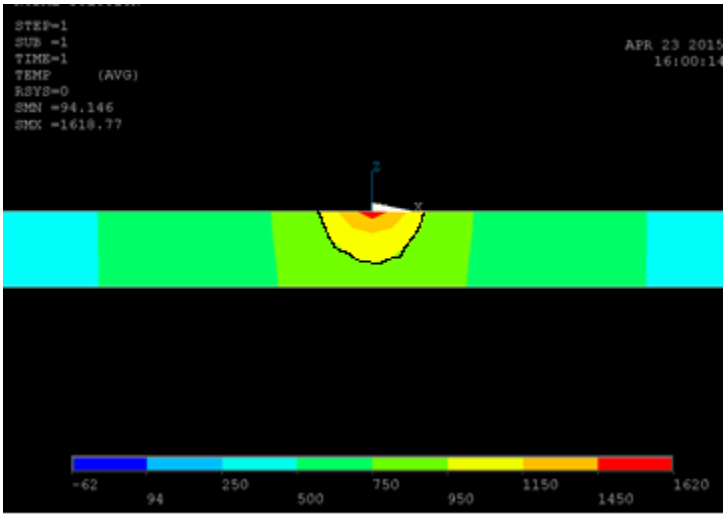

Figure 14: Close-up view of temperature distribution.

Area in red color is the melted zone, because temperature range of the red color region is above melting temperature of AISI 304 material (1450 C). The area in temperature range 950-1450 C is taken as heat affected zone. These are the measured parameter values.

Width of weld (W) = 0.45 mm

Depth of weld (D) =0. 125mm

Ratio (W/D) = 3.6

HAZ= 0.25mm

3.1.2 Second iteration

In the second iteration work piece area above the melting temperature is converted into liquid region and liquid metal properties are given as shown in figure 15. Solid and liquid

interface boundary condition is given at the place of interface. From now all the remaining iterations are run with both solid and liquid regions. Then again same boundary conditions are given and the model is finely meshed and same heat flux function is applied. Then the temperature distribution on the work piece is captured. The amount of power absorbed or absorptivity coefficient of work piece is taken as 54.27%, because from the second iteration, work piece is in solid + liquid phase (melting temperature). The figure 16 shows the 2nd iteration temperature distribution of work piece for 120W laser power.

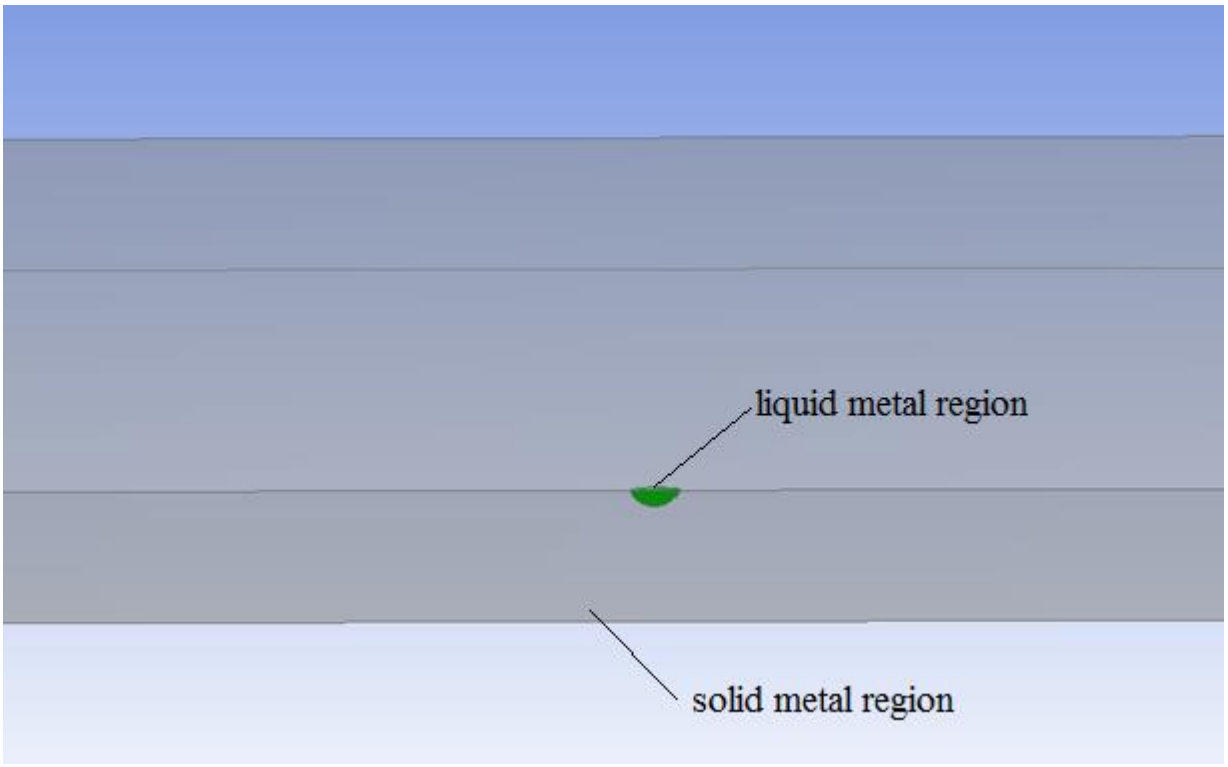

Figure 15: solid + liquid phase work piece.

The measured parameters for the 2nd iteration are:

Assumed Amount of power absorbed (or) absorption coefficient 54.2% (Liquid+ solid phase).

Width of weld (W) = 1.54 mm

Depth of weld (D) =0. 542mm

Ratio (W/D) = 2.21

HAZ= 1.53mm

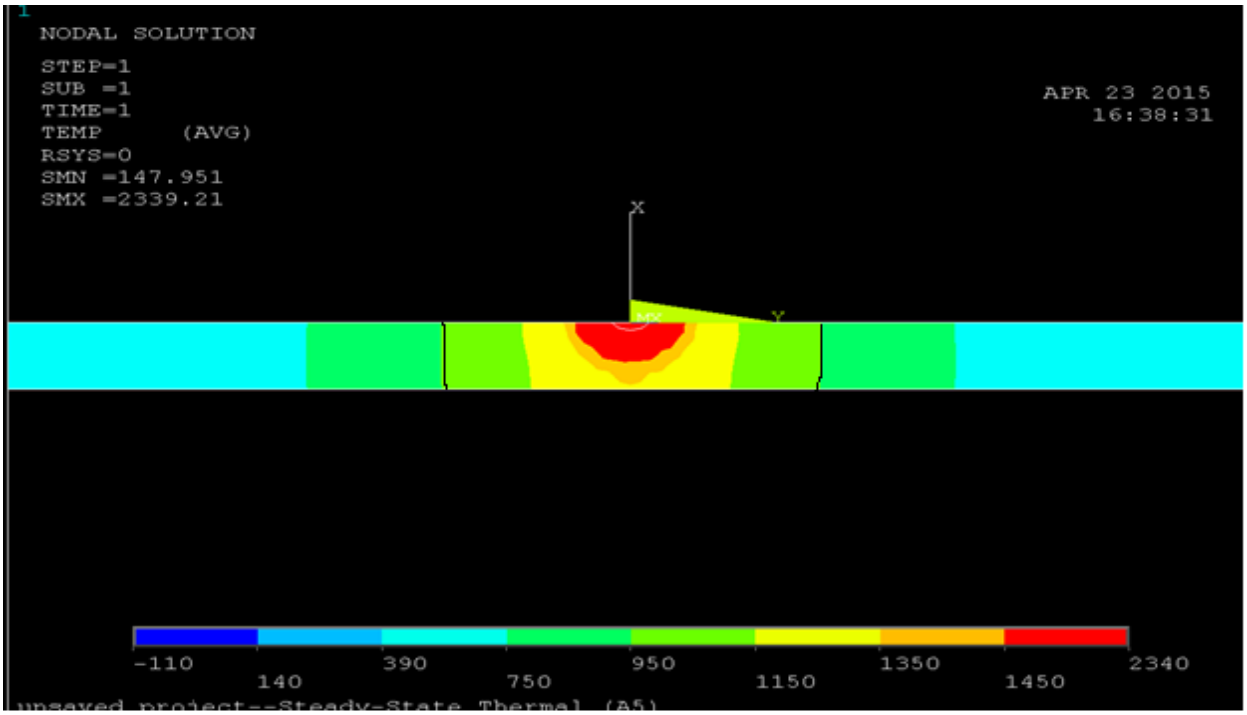

Figure 16: Steady state 2nd iteration temperature distribution on work piece for 120W laser power.

3.1.3 Third iteration:

Similarly in third iteration, area of the work piece above melting temperature is converted into liquid and same boundary conditions are applied. Simulation is performed and the temperature distribution is obtained. The figure 17 shows the temperature distribution of the work piece.

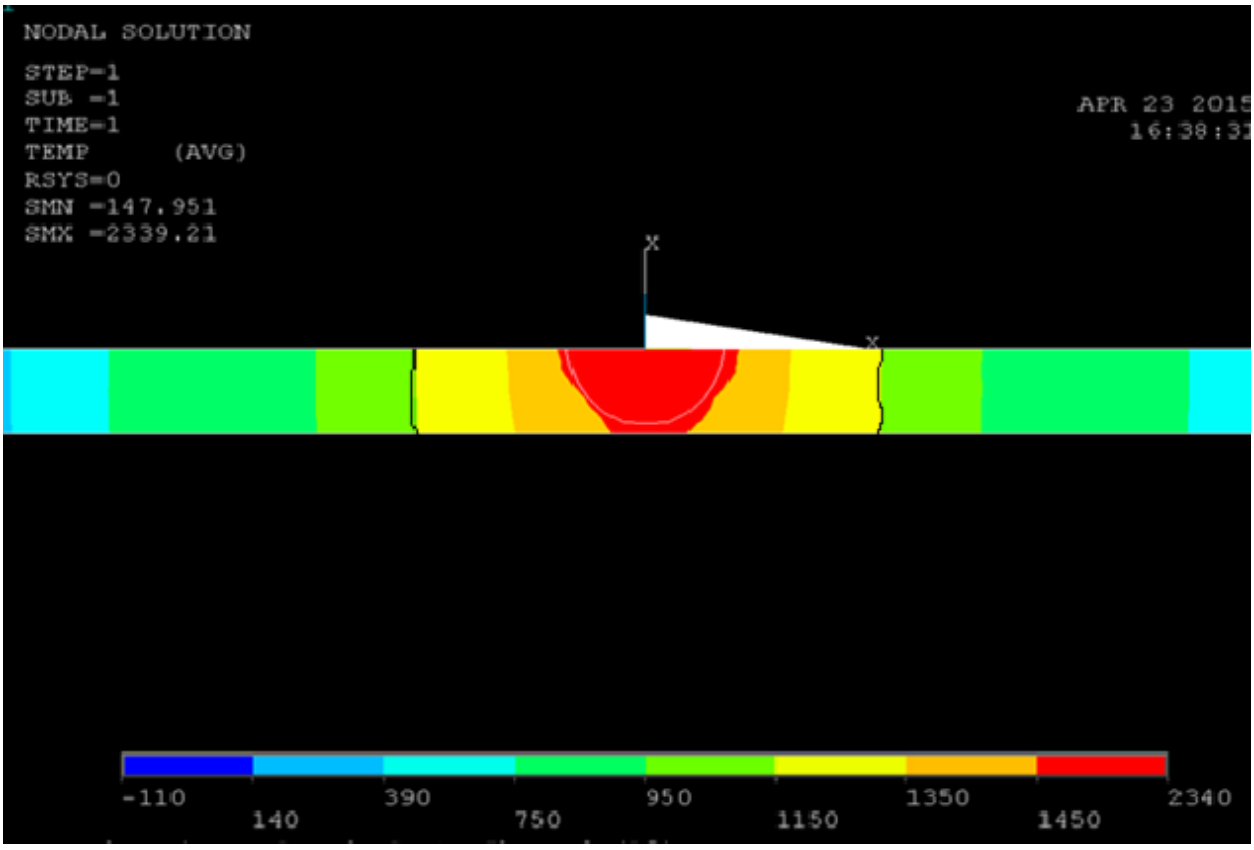

Figure 17: Steady state 3rd iteration temperature distribution on work piece for 120W laser power.

Assumed Amount of power absorbed 54.2%. (Liquid +solid phase)

Width of weld (W) = 1.48mm

Depth of weld (D) =1 mm

Ratio (W/D) = 1

HAZ = 1.95mm

3.2 Transient thermal analysis

Now the same simulation is modelled in the transient thermal system. Transient system is time dependent. Here we need to specify the run time for running the simulation. Properties like material properties, work piece model, heat source function and boundary conditions remains same as steady state. Each simulation is run till the convergent results are obtained.

3.2.1 First iteration

For the first iteration the work is at room temperature and it is in solid phase. So the coefficient of reflectivity is high. Absorptivity is taken as 31.7% and the heat flux is calculated based on that. All the boundary conditions remain same and simulation is done. The figure 18 and 19 shows the temperature distribution for the 1st iteration in transient analysis.

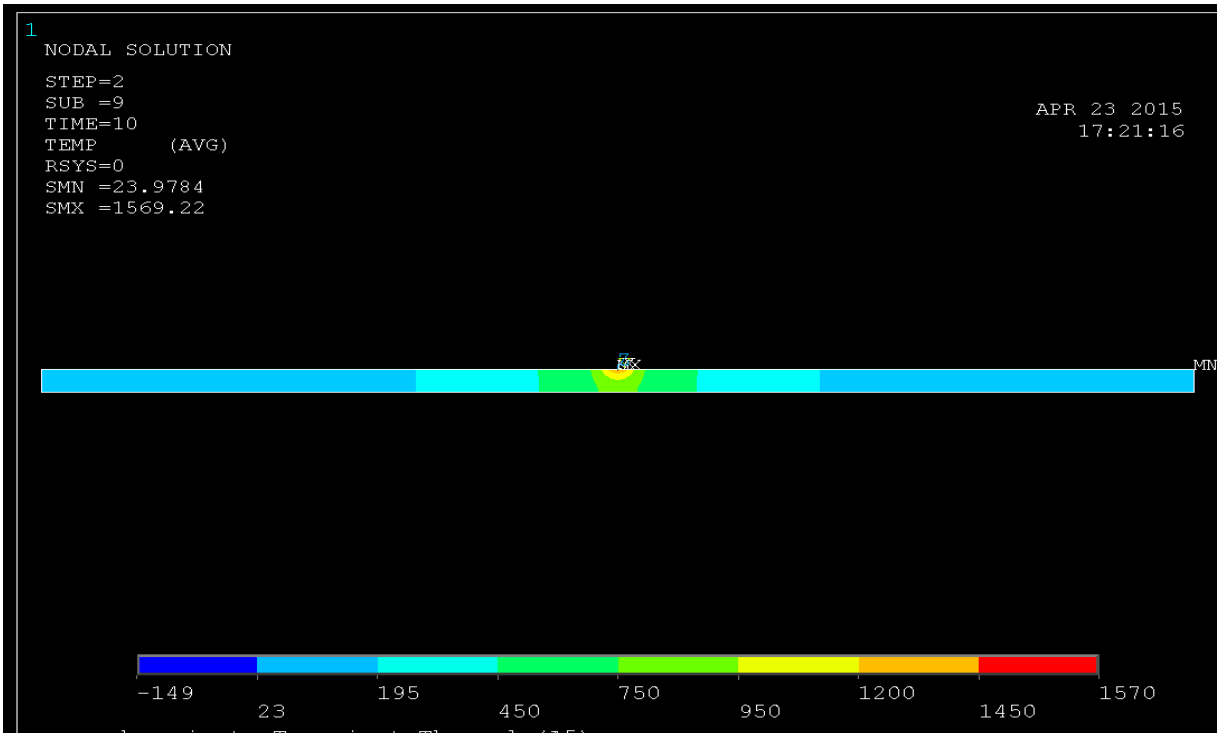

Figure 18: Transient 1st iteration temperature distribution on work piece for 120W laser power.

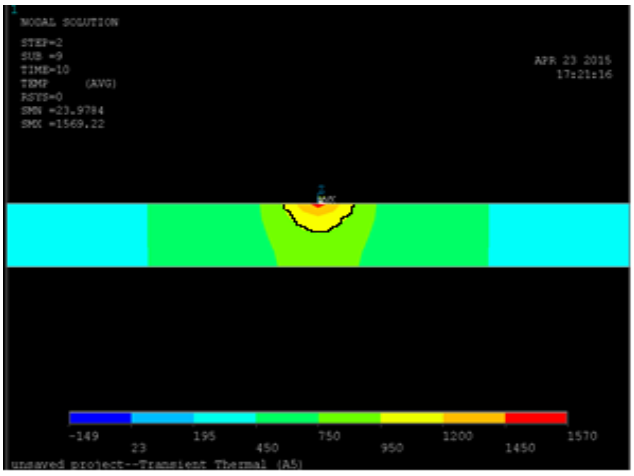

Figure 19: Close-up view of 1st iteration.

Once the simulation is performed the parameters like width of weld, depth of weld, HAZ are measured. The measured properties are

Absorption coefficient used = 31.7%.

Width of weld (W) = 0.25 mm

Depth of weld (D) =0. 08mm

Ratio (W/D) = 3.125

HAZ= 0.25mm

3.2.2 Second iteration

In the second iteration work piece area above the melting temperature is converted into liquid region and liquid metal properties are given as shown in figure 15. Solid and liquid interface boundary condition is given at the place of interface. From now all the remaining iterations are run with both solid and liquid regions. Then again same boundary conditions are given and the model is finely meshed and same heat flux function is applied. Then the temperature distribution on the work piece is captured.

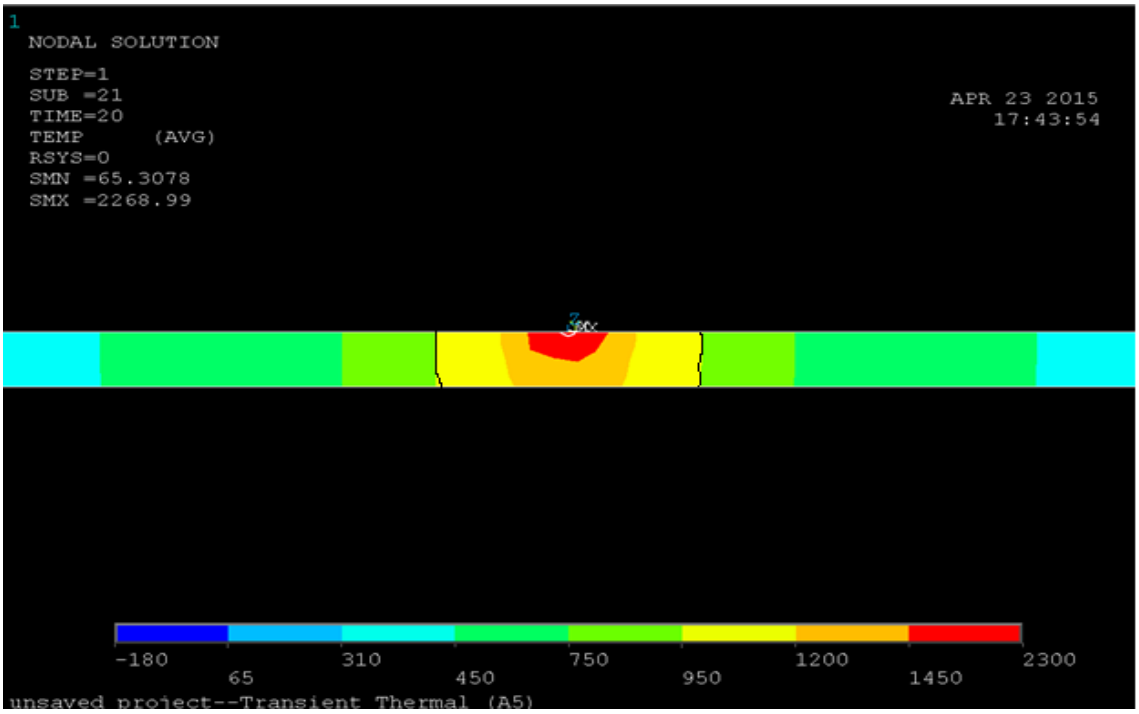

Figure 20: Transient 1st iteration temperature distribution on work piece for 120W laser power.

Measured parameters are:

Absorption coefficient used = 54.2%.

Width of weld (W) = 1.159 mm

Depth of weld (D) =0. 5mm

Ratio (W/D) = 2.38

HAZ= 1.42mm

3.2.3 Third iteration

In this iteration the area above the melting temperature in 2nd iteration is converted into liquid region and the simulation is performed keeping all other things constant. The temperature distribution on work piece is shown in figure 21.

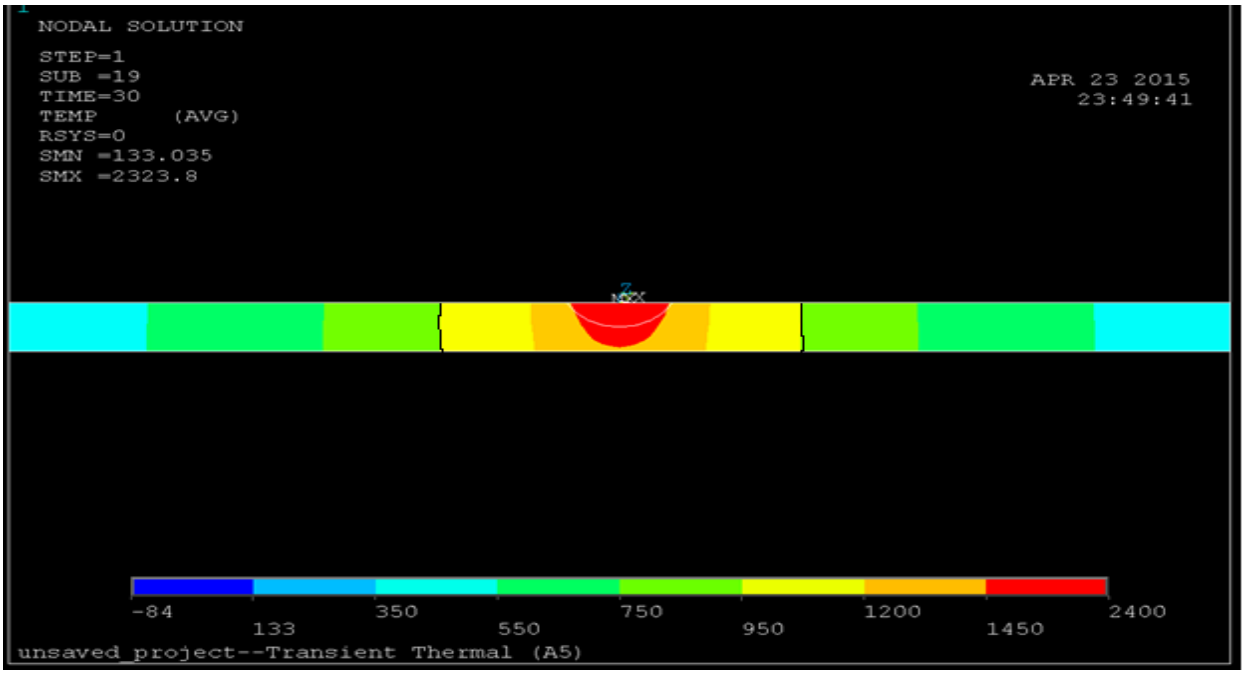

Figure 21: Transient 3rd iteration temperature distribution on work piece for 120W laser power.

The measured parameters are

Absorption coefficient used = 54.2%

Width of weld (W) = 1.437mm

Depth of weld (D) =0.883 mm

Ratio (W/D) = 1.63, HAZ = 1.4315mm

3.2.4 Fourth iteration

The area above melting temperature in 3rd iteration is converted into liquid region and the simulation is repeated again.

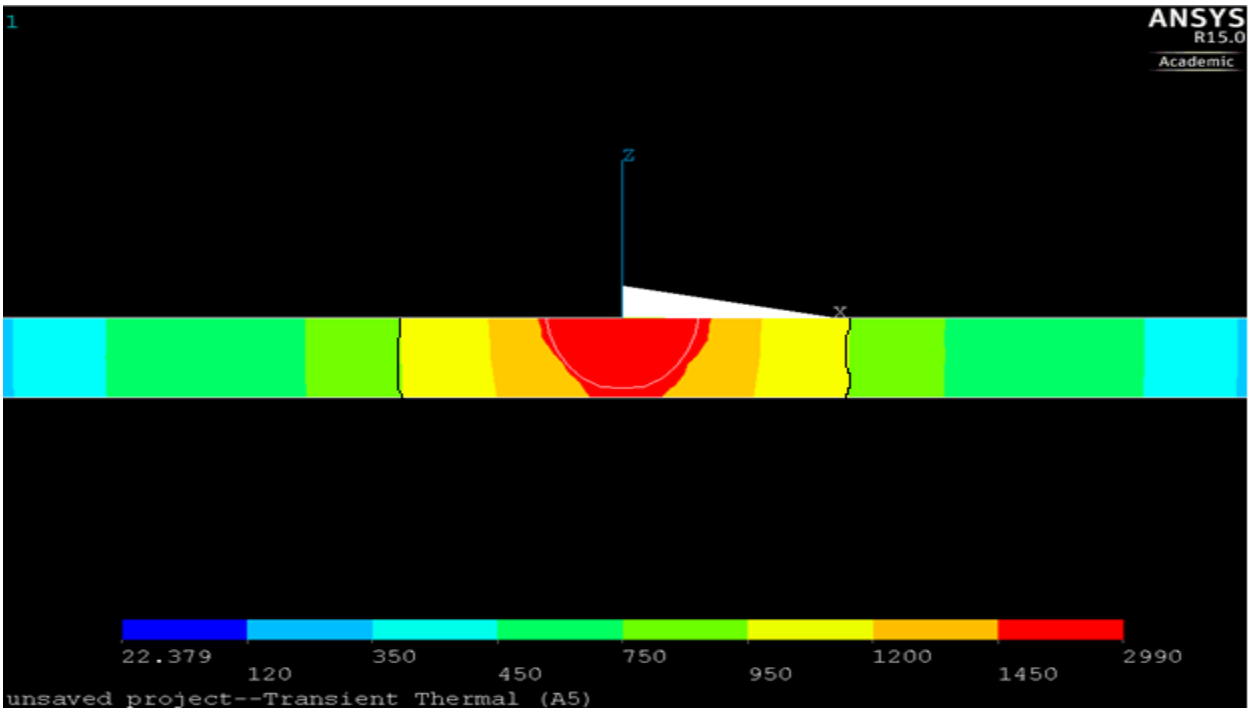

Figure 22: Transient 4th iteration temperature distribution on work piece for 120W laser power.

The measured parameters are

Absorption coefficient used = 54.2%

Width of weld (W) = 1.47mm, HAZ= 1.915mm

Depth of weld (D) =1 mm, Ratio (W/D) = 1.47

3.3 Keyhole formation

The keyhole formation in micro laser welding is simulated in Ansys. The development of keyhole at different steps is shown in following figure 23.

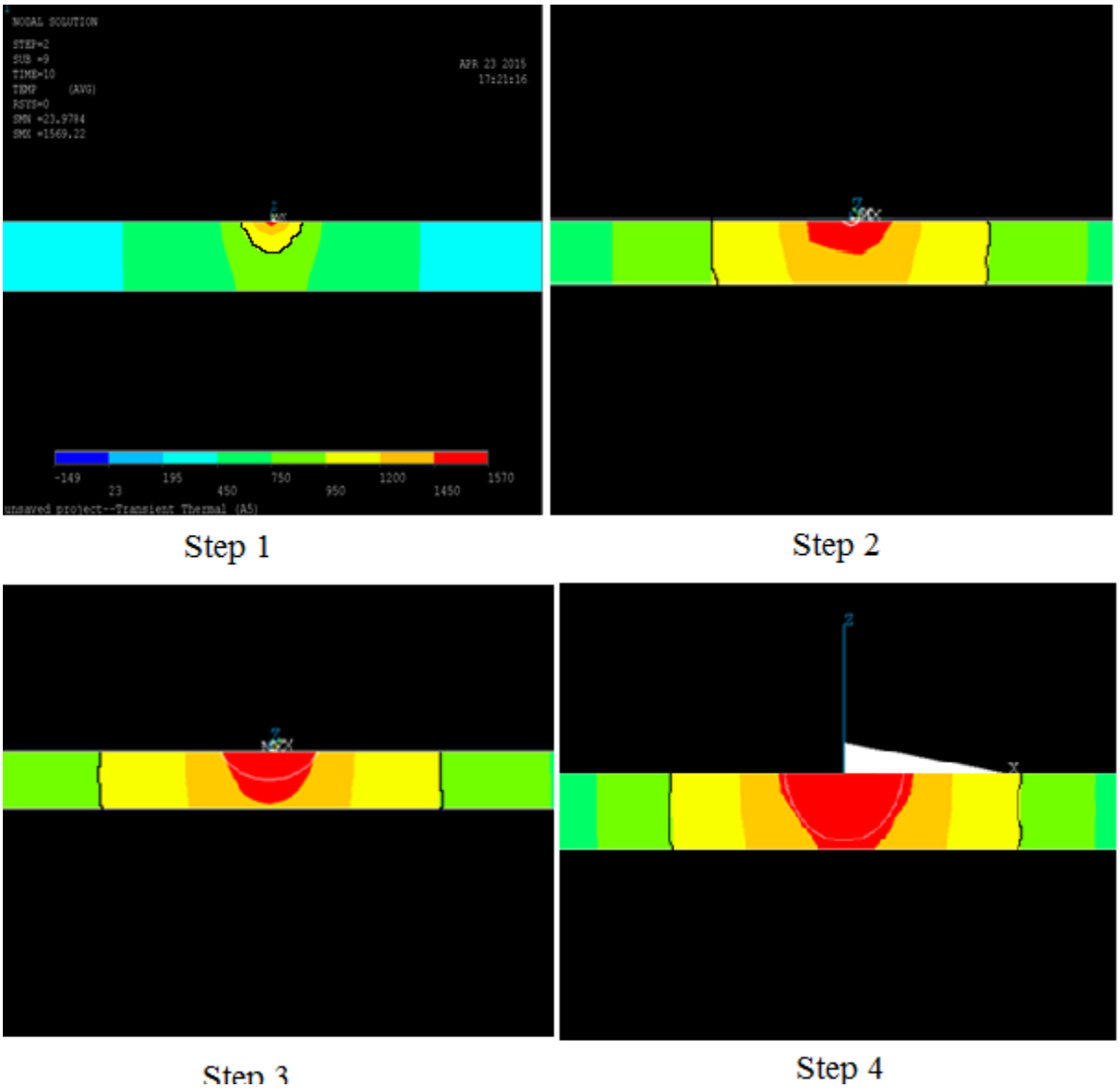

Figure 23: Keyhole development in micro laser welding at different time steps.

CHAPTER 4

RESULTS AND DISCUSSIONS

In this chapter all the observations and results are discussed such as

1. Comparison of steady state results with transient thermal results
2. Validation on simulated results with experimental results
3. Relations between the weld parameters bead width to depth ratio, intensity of laser beam and time of weld.

4.1 Comparison of steady state results with transient thermal results

The steady state and transient thermal analysis is performed for different laser power like 100W, 120W and 140W values. Then all the steady state and transient thermal weld parameters like width (W), depth of cut (D), Ratio (W/D) and HAZ are compared and the error percent is calculated. The below table 1 shows all the measured parameters of steady state and transient thermo-fluid models.

Table 1: simulated weld parameter results

	100W Steady	100W Transient	120W steady	120W Transient	140W steady	140W Transient
WIDTH(mm)	1.71	1.68	1.48	1.47	1.29	1.26
DEPTH(mm)	1	1	1	1	1	1
HAZ (mm)	1.8	1.76	1.95	1.915	2.1	2.05
RATIO	1.71	1.68	1.48	1.47	1.29	1.26

The results of steady state and transient thermo-fluid models are all most same with 1-2% error.

4.2 Validation on simulated results with experimental results

The simulated Ansys results are compared with the previous experimental results [10]. The experimental results are obtained from fiber delivered, flash-lamp pumped SLS 200 pulsed Nd: YAG laser. Nd: YAG means neodymium-doped yttrium aluminum garnet [10]. The specifications of Laser machine used are:

Table 2: Laser machine specifications [10]

Type:	Pulsed Nd :YAG – solid state laser
Pulse frequency:	0.1-1000Hz
Wave length:	1064 nm
Incident Beam diameter:	0.3 mm
Optical fiber diameter:	50 - 400µm
Pulse energy:	50-120J
Pulse duration:	0.1-20 MS

The experiment has been performed with all most same input parameters same as simulated (Work piece specifications, power, radius of beam and etc.). The experimental weld parameters such as width, depth of weld and HAZ are measured. The below table 3 shows the comparison between experimental and simulated weld are shown.

Table 3: Comparison with experimental work and simulated values

Laser Beam Power In Watts	Experimental Ratio (Width/Depth)	Simulated Ratio (Width/Depth)	Experimental HAZ(mm)	Simulated HAZ(mm)
35W	4.6	4.7	0.37	0.386
30W	3.8	3.65	0.3	0.31

The overall percentage of error between the simulated and experimental values is calculated to be less than ±2-3%. In general many researches claim that only single phase models

have the accuracy of ±5%. This shows that the present simplified assumption of liquid and solid phase of material yields better results than the only conduction type welding.

4.3 Observations between the weld parameters

Based on the measured values the relations between the weld parameters are studied. Here are the some of the observations.

4.3.1 Bead width to Depth Ratio Vs Intensity

It is observed that when intensity of laser beam (laser beam power) increases the weld bead width to bead depth ratio decreases (W/D). The table 4 and graph shows the comparison between beam intensity and weld bead width to depth ratio.

Table 4: Bead width to Depth Ratio Vs Intensity

Beam Intensity in watts	Bead Width to Depth ratio
30	4.7
35	3.65
100	1.6
120	1.48
140	1.26

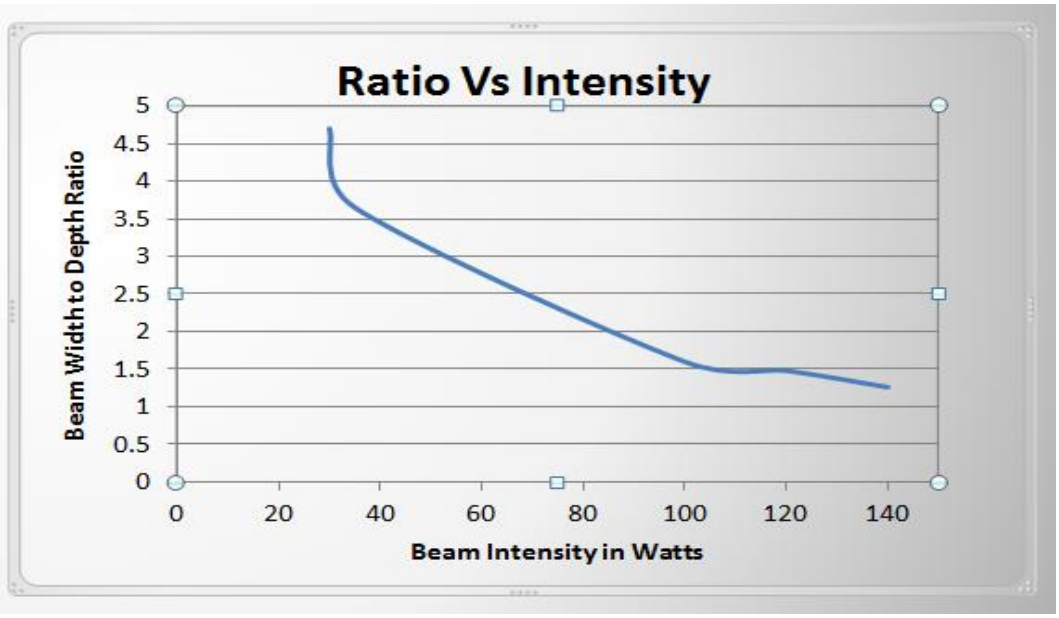

Figure 24: Bead width to Depth Ratio Vs Intensity.

4.3.2. Bead width to Depth Ratio Vs Time of weld

It is observed that time of weld is inversely proportional to the bead width to depth ratio. The comparison is shown in below table 5 and the graph.

Table 5: Bead width to Depth Ratio Vs Time of weld

Iteration number	Bead Width to Depth ratio
1	3.125
2	2.38
3	1.63
4	1.47

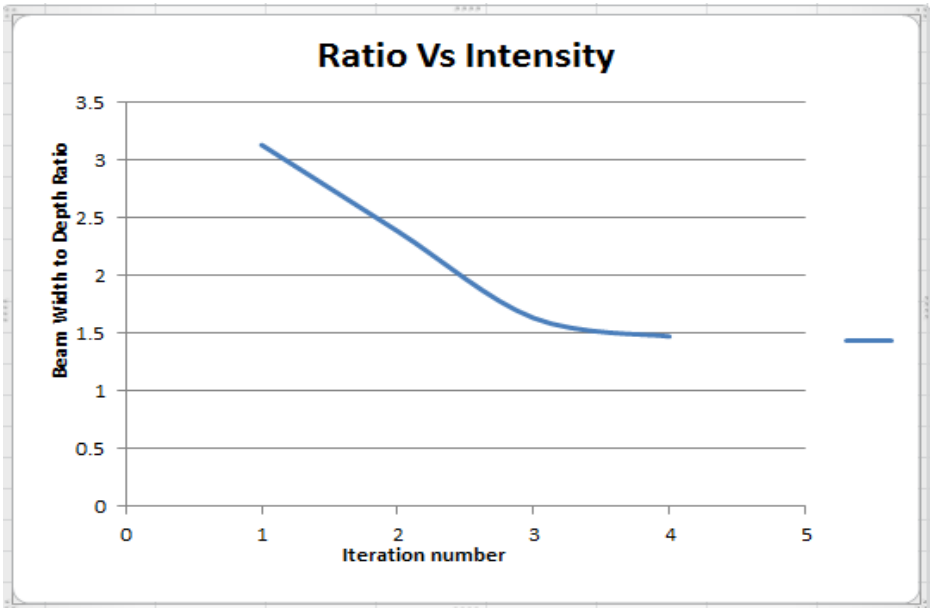

Figure 25: Graph between Bead width to Depth Ratio and Time of weld.

4.3.3. Beam intensity Vs Depth ratio

From the below table 6 and graph it is observed that, with increase in intensity of laser beam (Laser beam power) the weld HAZ also increases.

Table 6: Beam intensity Vs Depth ratio

Beam Intensity in watts	Heat effected zone(mm)
30	0.31
35	0.386
100	1.8
120	1.95
140	2.1

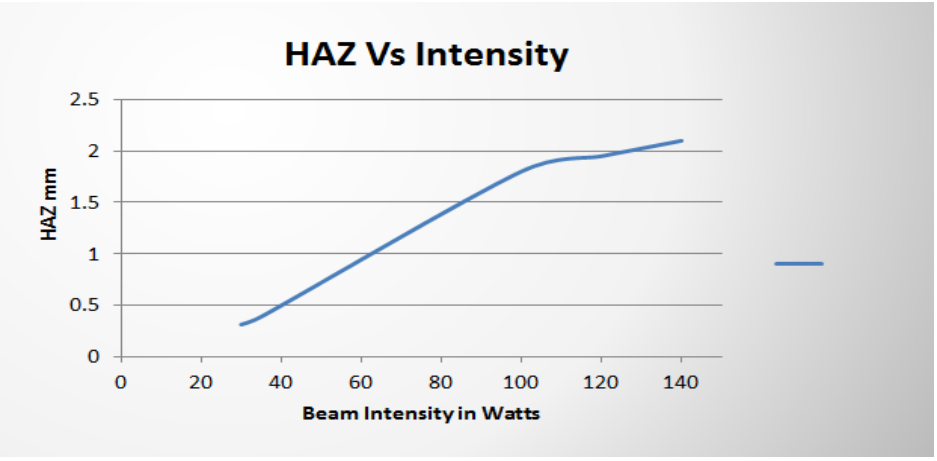

Figure 26: Graph between HAZ and Intensity.

CHAPTER 5

CONCLUSION

The 3D simplified thermo-fluid model is simulated and the steady state and transient analysis is done. The obtained simulated values are validated with the experimental values. Finally following conclusions are made.

- A 3D steady state and transient thermo-fluid models of micro laser welding are developed separately in finite element analysis software Ansys and Ansys WB.
- The model is developed considering the two phase's liquid metal and solid metal in simplified liquid phase assumption.
- Development of key hole is observed.
- The results of steady state and transient thermo-fluid models are all most same (1-2% error).
- The results obtained from the simulation are compared with those from the experimental data form laser welding and it is observed that the results of numerical analysis (FEM) are in good agreement with experimental results, with an overall percentage of error estimated to be within ±2-3%.
- The assumption considering the two phase's liquid metal and solid metal i.e. simplified liquid phase assumption has better results compared to only conduction type welding with error percentage of ±5%.
- It is observed that with increase in intensity of laser beam (Laser beam power) the weld bead width to Depth ratio decreases.
- Time of weld is inversely proportional to the bead width to height ratio.

- With increase in intensity of laser beam (Laser beam power) the weld HAZ also increases.

REFERENCE

[1]. Welding definition, Wikipedia, https://en.wikipedia.org/wiki/Welding

[2]. Koo, B.S., 2013, "Simulation of Melt Penetration and Fluid Flow Behavior during Laser welding". Ph.D. thesis, Lehigh University, Thesis and Dissertations, pp. 1319, http://preserve.lehigh.edu/etd/

[3]. Jay Eastman, 2015, "Conduction Mode vs. Keyhole Mode Laser Welding," Online Article, http://ewi.org/conduction-mode-vs-keyhole-mode-laser-welding/

[4]. Xie, J., and Kar, A., 1999, "Laser Welding of Thin Sheet Steel with Surface Oxidation," Welding Journal Research Supplement, pp 343-348.

[5]. De, A., Maiti, K., Wash, C.A., Bhadeshia, and H.K.D.H., 2003, "Finite Element Simulation of Laser Spot Welding," Article in Science and Technology of Welding & Joining 8 (5), 377-384.

[6]. Siva Shanmugam, N., Buvanashekaran, G., and Sankaranarayanasamy, K., 2009, "Finite Element Simulation of ND:YAG Laser Lap Welding of AISI 304 Stainless Steel Sheets," Research Article ISBN: 978-1-61804-142-5, Department of Mechanical Engineering, National Institute of Technology, Tamil Nadu, India.

[7]. Katiar, K., 2012, "Dynamic Simulation of Temperature Field in Nd:YAG laser Welding Using Finite Element Analysis," M.Tech. Thesis, National Institute of technology, Rourkela.

[8]. Stritt, P., Weber, R., Graf, T., Muller, S. and Ebert, C., 2011, "Utilizing Laser Power Modulation to Investigate the Transition from Heat-Conduction to Deep-Penetration Welding," Proceedings of the Sixth International WLT Conference on Lasers in Manufacturing, Munich, Germany, Physics Procedia, Volume 12, Part A, pp 6-786.

[9]. Cho, H., 2011, "Determination of Effects of Laser Parameters to Micro-Laser Drilling by Experiment and Simulation," M.S. Thesis, Department of Mechanical Engineering, Northern Illinois University, Dekalb, Illinois.

[10]. Aditya, C., 2015, "Optimization of Laser Welding in Pulsed Nd:YAG Laser using ANSI 304 Stainless Steel," M.S. Thesis, Department of Mechanical Engineering, Northern Illinois University, Dekalb, Illinois.

[11]. Sekhar Babu, A. N. and Lakshmana Kishore, T., 2012, “Finite Element Simulation of Hybrid Welding Process for Welding 304 Austenitic Stainless Steel Plate,” International Journal of Research in Engineering and Technology, ISSN: 2319-1163.

[12]. Charles, J., Mithieux, J.D., Santacreu, P.O. and Peguet, L., “The Ferritic Stainless Steel Family: The Appropriate Answer to Nickel Volatility?” ArcelorMittal Stainless, France, http://www.euro-inox.org/pdf/map/paper/Nickel_Volatility_EN.pdf